Erzincan Üniversitesi
Fen Bilimleri Enstitüsü Dergisi
2022, 15(2), 622-635
ISSN: 1307-9085, e-ISSN: 2149-4584
Araştırma Makalesi

Erzincan University
Journal of Science and Technology
2022, 15(2), 622-635
DOI: 10.18185/erzifbed.1130305
Research Article

Breast Tumor Detection and Classification Based on Microwave Imaging

Emin Argun Oral[1,2*], Alan V. Sahakian[3]

[1]Ataturk University, Department of Electrical and Electronics Engineering, Erzurum, 25240 Turkey
[2]Ataturk University, High Performance Computing Application and Research Center, Erzurum, 25240 Turkey
[3]Northwestern University, Department of Biomedical Engineering and Department of Electrical and Computer Engineering, Evanston, IL, 60208 USA

Geliş / Received: 15/06/2022, Kabul / Accepted: 15/08/2022

Abstract

Limitations caused by traditional breast cancer detection and screening techniques have initiated researchers to investigate alternative solutions. This study examines the use of a microwave-based approach for tumor detection in breast tissue and related tumor type classification using matched-filtering. Radar-like confocal microwave imaging (CMI) method constructs the foundation of such tumor detection approach. In particular, a microwave pulse is first transmitted, then back-scattered pulses are collected. All major reflective sites in the breast tissue are detected by repeating this procedure on a microwave pulse transmission-reception grid, aligning captured signals in-time to focus on a particular region in the breast tissue and superimposing such time-shifted signals to improve signal-to-clutter level. In the observed signals, clutter is originated by the heterogeneity of the breast tissue while signal is originated by a tumor site as a function of its water content.
All calculations, in the study, were performed computationally in terms of a 3D Finite-Difference Time-Domain (FDTD) simulation models. For the antenna system, two cross-polarized resistively loaded bow-ties antennas were used in the computational model, and the tumor site was modeled using five different sizes and morphologies. Matched-filtering, on the other hand, was performed by matching such obtained observations with that of a homogenous breast tissue, namely clutter-free model. Performance of the proposed approach was tested for two different antenna array resolutions, and it was observed that this parameter is important for successful detection and classification of a tumor-site in a realistic heterogeneous breast tissue model.

Keywords: Confocal microwave imaging, 3D FDTD, matched-filtering, spherical tumor, cylindrical tumor

Mikrodalga Görüntüleme Tabanlı Meme Kanseri Belirleme ve Sınıflandırma

Öz

Geleneksel meme kanseri tespit ve tarama tekniklerinin sahip olduğu sınırlamalar, araştırmacıları alternatif çözümleri araştırmaya teşvik etmiştir. Bu çalışmada, meme dokusunda tümör tespiti için mikrodalga tabanlı bir yaklaşım ve ilgili tümör tipi sınıflandırması için uyumlu-filtre kullanımı incelemektedir. Radar benzeri konfokal mikrodalga görüntüleme (confocal microwave imaging - CMI) yöntemi, bu tümör algılama yaklaşımının temelini oluşturmaktadır. Bu yaklaşımda önce bir mikrodalga darbesi iletilir ve ardından geri saçılan darbeler kaydedilir. Meme dokusundaki tüm büyük yansıtıcı bölgeleri belirlemek için bu prosedür; bir mikrodalga darbe gönderme-alma ızgarasında tekrarlanır, meme dokusundaki belirli bir bölgeye odaklanmak için kaydedilen bu sinyaller zamanda hizalanır ve işaret-gürültü oranını iyileştirmek için bu ötelenmiş sinyaller üst üste bindirilir. Kaydedilen işaretlerdeki gürültü bileşeni, meme dokusunun heterojenliğinden kaynaklanırken, sinyal bileşeni su muhteviyatının fonksiyonu olarak tümör bölgesinden kaynaklanır.
Çalışmadaki tüm hesaplamalar, 3B Zaman Uzayı Sonlu Farklar (Finite Difference Time Domain - FDTD) simülasyon modelleri şeklinde hesaplamalı olarak gerçekleştirildi. Anten sistemi için hesaplama modelinde iki adet çapraz polarize direnç yüklü papyon anten (bow-tie antenna) kullanılırken, tümör bölgesi beş farklı boyut-morfoloji kullanılarak modellendi. Öte yandan uyumlu-filtreleme sinyalleri için gürültü içermeyen homojen meme dokusu kayıtları kullanıldı. Önerilen yaklaşımın performansı iki farklı anten dizisi çözünürlüğü için test edildi ve gerçekçi bir heterojen meme dokusu modelinde test tümör bölgesinin başarıyla tespit edilip, sınıflandırılmasında bu parametrenin önemli olduğu gözlemlendi.

Anahtar Kelimeler: Konfokal mikrodalga görüntüleme, 3B FDTD, uyumlu süzgeç, küresel tümör, silindirik tümör

***Corresponding Author:** eminoral@atauni.edu.tr
Emin Argun Oral, https://orcid.org/0000-0002-8120-9679
Alan V. Sahakian, https://orcid.org/0000-0003-3090-0328

1. Introduction

Breast cancer is very common among women worldwide. A death rate of 15% was reported by the American Cancer Society in 2021 [1], and lack of awareness results in even a higher mortality rate for men. It is fundamental to detect breast cancer at an early stage for a successful treatment. For this purpose, the X-ray mammography, the magnetic resonance imaging (MRI) and the ultrasound scanning are the most common clinical imaging and detection modalities, but they have some disadvantages and limitations such as use of ionizing radiation, being uncomfortable or expensive as well as requiring experienced operators. This motivates researchers to investigate new imaging approaches [2-4]. Among these, microwave imaging received significant attention due to its harmless radiation, low cost, and ease of use.

Use of electromagnetic waves at microwave frequencies is considered for diagnosis, therapy as well as imaging in medicine. Of these, noninvasive imaging of soft tissues has been proposed, and three modalities have been studied for microwave based breast cancer detection. These can be categorized as passive [5-6], active [7-10] and hybrid [11] techniques. Passive methods utilize a radiometry device to compare the temperature difference between healthy and malignant tissues. In hybrid techniques, on the other hand, illuminated and detected signals have different origins. There are a variety of active microwave imaging techniques, which are of our concern in this study, including tomography and radar based methods. In the former, electrical parameters of breast tissue are constructed through inverse scattering approaches while an ultra-wideband microwave illumination and related back-scattered signals are used to locate a tumorous site in the region of interest in the latter. Hagness et al. [12, 13] proposed such microwave-based breast cancer detection approach, named as confocal microwave imaging (CMI) [14], utilizing backscatter signals to locate major microwave scatter structures in the examined tissue. This approach is based on the use of electrical properties' contrast between normal breast tissue and tumorous regions and differs from others such as tomographic microwave imaging which utilize transmissions to map dielectric properties [15]. In this sense, malignant tumors' and different surrounding biological structures' electrical properties were studied in [16], it was reported that the water content is responsible for such contrast up to microwave frequencies [17], and this difference was also suggested for tumor detection [16]. Since then, there have been studies of microwave imaging for breast cancer detection.

Much of the work to date has involved computational studies based on 2D planar [13], cylindrical [18] and a few 3D spherical [19] FDTD models considering 5-15 mm size tumors [20-22] as well as CMI based experimental studies [12, 13, 23]. These studies are performed in 1-15 GHz frequency band, mostly utilizing 3-6 GHz frequency range. There are only a few computational models with tumor sizes less than 4 mm [24-25]. Most of the obtained results highlight a major problem of skin backscatter or initial reflection below the skin layer. They are larger in magnitude compared to the in-tissue scattered signals, masking them partially since they occur earlier in time. Some calibration algorithms are proposed to remove these skin related reflections from the recorded signals [18], [26] based on some assumptions. As an alternative approach, it is proposed, in the current study, to define all candidate locations for a

possible tumor in the tissue first, and then to decide whether the related back-scatter signals qualify for tumor existence or not based on a matched-filtering test step.

The paper is organized as follows. An overview of the proposed computational model and method is presented in Section 2. In Section 3, obtained results along with corresponding discussion are discussed. And finally in Section 4, all the important points are summarized in the conclusion.

2. Material and Methods

A. Computational Model

The Finite Difference Time Domain (FDTD) based computational model of the study is shown in Figure 1(a). This 3D model simulates the interaction of an antenna system with a breast structure. The whole FDTD model is terminated on both ends of each dimensions by two perfect matched layer (PML), backed with perfect electrical conductor layer (PEC) to terminate the simulation model. The antenna-breast interaction model is composed of three layers, namely the antenna layer, the skin layer and the breast structure, as shown in Figure 1(b). Of these, the antenna layer hosts two resistively loaded bow-tie antennas, one for transmission and the other for reception, in a cross-polarization setup to avoid from cross-talk between the two. The breast structure, on the other hand, is separated from the antenna layer by the skin layer and contains a tumorous site inside.

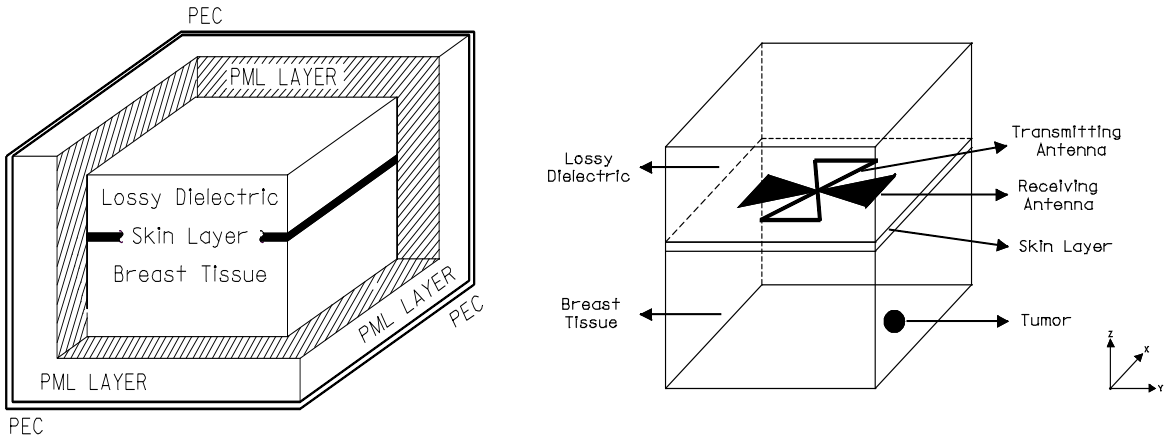

(a) (b)

Figure 1. Computational model of the study: (a) 3D FDTD components, (b) Microwave radiation components

In the model, the breast structure is represented by an 8 cm x 8 cm x 5 cm dielectric block, of which each 5 mm^3 chunk is designated with varying electrical parameters. These parameters are considered to be uniformly distributed in 0.4±10% S/m and 9±10% ranges for conductivity and relative permittivity, respectively. That of the 1.7 mm thick skin layer is 4 S/m and 36, respectively. These parameters are consistent with those parameters of the study in Hagness et al. [13]. Note that the antenna layer is a lossy dielectric material covering the whole antenna system and matched to the average electrical parameters of the breast structure. The last component of the model is a spherical-tumor site in 5 mm diameter submerged in the breast structure with conductivity and relative permittivity of 7 S/m and 50, respectively.The

microwave radiation employed in the study is a differentiated Gaussian pulse centered at 6 GHz. Following the pulse delivery through the transmission antenna, corresponding reflections are collected by the transmitting antenna, and this procedure is repeated on an antenna-array with resolutions of 8 mm and 16 mm.

B. Tumor Detection Algorithm

Basis of proposed tumor detection algorithm is defined by CMI. Here, a microwave pulse propagation through transmission antenna and corresponding reception through receiving antenna is implemented on all antenna-array locations. The captured reception is composed of possible tumor-related microwave pulse reflection, namely signal to be detected, and breast tissue heterogeneity induced back-scattering, namely the clutter. After intercepted signals are collected on all antenna-array locations, a Shift&Sum procedure is employed. Here, distance between the antenna system location as well as corresponding round-trip time-delay are both calculated considering a "candidate tumorous site" in the breast tissue, and this procedure is repeated for all antenna-array locations for same "candidate tumorous site". To improve the signal-to-clutter ratio of the observations, all captured signals are aligned to superimpose the potential reflections of the "candidate tumorous site", namely signal, their magnitudes are adjusted using a set of weighting coefficients, and finally they are combined. In this Shift&Sum algorithm, weighting coefficients are defined considering the propagation attenuation together with radial spreading of the transmitted pulse and size of the reflective shell housing the possible tumorous site. Here, the use of coefficients is different from [26] in the sense that instead of the equalizing the possible tumor reflections magnitudes, Shift&Sum algorithm equalizes the clutter level. As a result, the obtained Shift&Sum procedure output is not adjusted for the attenuation of the reflected signal but instead equalized for back scattering to better improve the signal-to-clutter level. The corresponding pseudo code for Shift&Sum procedure is shown in Algorithm 1.

Algorithm 1

```
OUTPUT Shift&Sum process out for all 3D breast pixels
// X, Y, Z number of pixels in the breast region (defined for x, y and z axes)
// M, N number of antenna array locations on the antenna plane (defined for x and y axes)

begin Shift&Sum
for i=1 to X do
for j=1 to Y do
for k=1 to Z do
        for a_x=1 to M do
        for a_y=1 to N do
                calculate round trip distance between (i,j,k) and (a_x, a_y) points
                calculate corresponding d_t travel time in the breast tissue
                use d_t to time shift antenna signal observed at (a_x, a_y) location
                compensate antenna array observation for attenuation
        end, end
SS(i,j,k)=average all shifted and compensated antenna array observations
end, end, end
return SS
end
```

Following this procedure, observed signals captured on the receiving antenna along with corresponding energy terms are calculated for all in-breast candidate points. In doing so, only the second-half of the observation window around the time-origin at which possible tumor

related reflections reside is utilized owing to the fact that earlier back-scattered pulses before the tumor related reflections have stronger magnitude in the first-half of this window compared to the second-half resulting in low signal-to-clutter ratio. At the end, dominant energy terms among all gathered in-breast candidate points construct the major microwave scatter mapping of the breast tissue. These major sites with high magnitude are considered as the possible tumor site and processed through a matched-filtering step for tumor type classification. Note that the transmitted differentiated Gaussian pulse is utilized here so that the observed tumor related reflections have odd symmetry in the study. This information is also considered in the tumor detection algorithm to eliminate some in-breast candidate points for tumor existence. That is Shift&Sum signals' polarization with high deviation from odd symmetry is excluded for tumor type classification.

C. Matched-Filtering

Once the major reflective sites in the breast tissue are detected, they are examined through matched-filtering to classify them as non-tumor related, in other words residue of a major back-scatter, or one of the filter bank signals, namely 2.5 mm, 5 mm and 7.5 mm diameter spherical-tumors or 6 mm long cylindrical-tumors with 3 mm and 4.2 mm diameters. For that, filter bank matching signals are obtained for computational FDTD model using a homogenous breast tissue with related tumor structure embedded. In doing so, matching signals are obtained using in-breast candidate points' Shift&Sum signals in the second-half of the observation window as previously explained.

As a final step, Shift&Sum procedure output signal, obtained for a candidate tumor site, is run through the match-filter bank. The corresponding matched-filter bank outputs' maxima along with their times are inspected to classify the type of the tumor, located on this site.

3. Results and Discussion

A. Tumor Back-scatter Observations in Homogenous Breast Model Results

Different morphologic and size of tumors were first implemented in a homogenous breast model and the resulting antenna observations were captured. This data was then fed into Shift&Sum algorithm to obtain the simulation output for an ideal case where no interfering clutter exists. In other words, homogenous breast tissue simulation data of breast-antenna system model were processed through the Shift&Sum algorithm. This obtained data, presented in this sub-section, was then utilized as the reference to measure the performance of matched-filtering classification of any possible breast tumors for a realistic heterogeneous breast model with an embedded tumor.

Five different tumors, all embedded in the breast tissue at a depth of 3 cm below the center of the antenna layer, were utilized to gather the reference for all-homogenous breast model data. These are 2.5 mm, 5 mm and 7.5 mm diameter spherical-tumors as well as 6 mm long

cylindrical-tumors with 3 mm and 4.2 mm diameters. Normalized to its magnitude Shift&Sum procedure output signal of the antenna-array observations for 5 mm diameter spherical-tumor is shown in Figure 2. Please note that the observed signal in this figure is centered in time to the transmitted differentiated Gaussian pulse origin.

Similar observations for the remaining tumor types are given in Figure 3 and 4. In both figures, all magnitudes are also normalized to the 5 mm diameter spherical-tumor simulation signal magnitude for computational purposes.

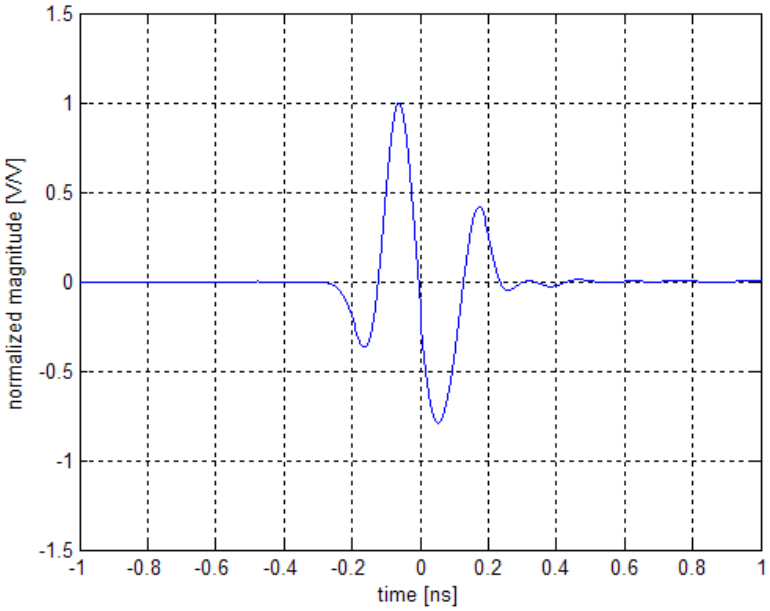

Figure 2. Normalized Shift&Sum algorithm output signal of the antenna-array observations obtained for a 5 mm diameter spherical-tumor at a depth of 3 cm in the breast model.

The output of Shift&Sum algorithm is a function of the tumors' physical sizes as well as electrical parameters, namely their scattering cross-sections. Since the electrical parameter variation of the tumors is not as significant as their shape for tumor classification point of view, all tumor structures, utilized in this study, are modeled using the same reported electrical parameters ($\sigma = 7$ S/m and $\varepsilon r = 50$) for all different tumor morphologies.

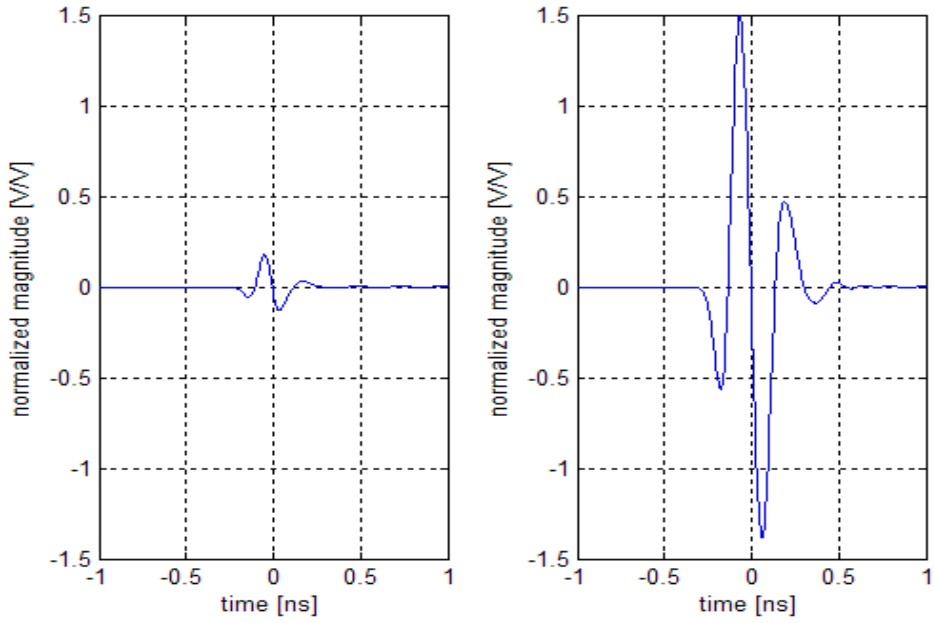

(a) (b)

Figure 3. Normalized Shift&Sum algorithm output signals for spherical tumors: (a) 2.5 mm diameter spherical-tumor, (b) 7.5 mm diameter spherical-tumor

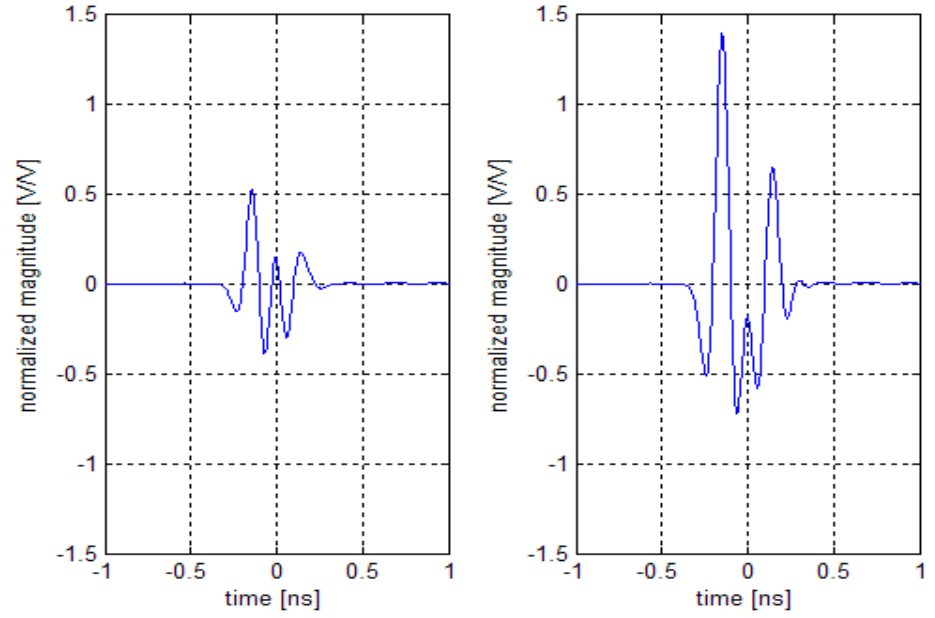

(a) (b)

Figure 4. Normalized Shift&Sum algorithm output signals for cylindrical tumors: (a) 3 mm diameter cylindrical-tumor, (b) 4.2 mm diameter cylindrical-tumor

B. Tumor Detection in Heterogeneous Breast Model Results

First step of the tumor morphology classification is the detection of the tumor site within the breast tissue model. For that a quadruple-symmetric heterogeneous model in the x-y plane for reduced computational load was constructed with a tumor site buried inside, and the simulation results were obtained. Obtained results are presented in this sub-section.

The tumor structure, included in the experimental model, is a single spherical-tumor with 5 mm diameter. It is embedded 1.30 cm underneath the skin layer of the breast tissue with an offset of 1.25 cm from the model center point, yielding a total depth of 3 cm from the antenna-array plane. Corresponding tumor detection algorithm results are shown in Figure 5, both for x-y and y-z planes. The x-y plane detection clearly points the exact tumor location, while y-z plane detection suggests two separate candidate locations. Of these, one is 3 cm below the center point, the true tumor location, and the other, a false location, is close to the antenna-array surface. These two tumor candidate locations were examined through the matched-filtering to evaluate tumor existence and its class, if exists. Note that all FDTD simulations were performed in one quadrant, upper-left, of the simulation model considering the symmetry over x and y-axes to reduce the computation time, bearing in mind the spatial resolution of 8 mm. This symmetry assumption is evident in both reconstructed images.

C. Matched-Filtering Results

The fundamental approach for tumor classification in terms of processing the back-scattered signal is matched-filtering, and the corresponding results are presented here. For comparison

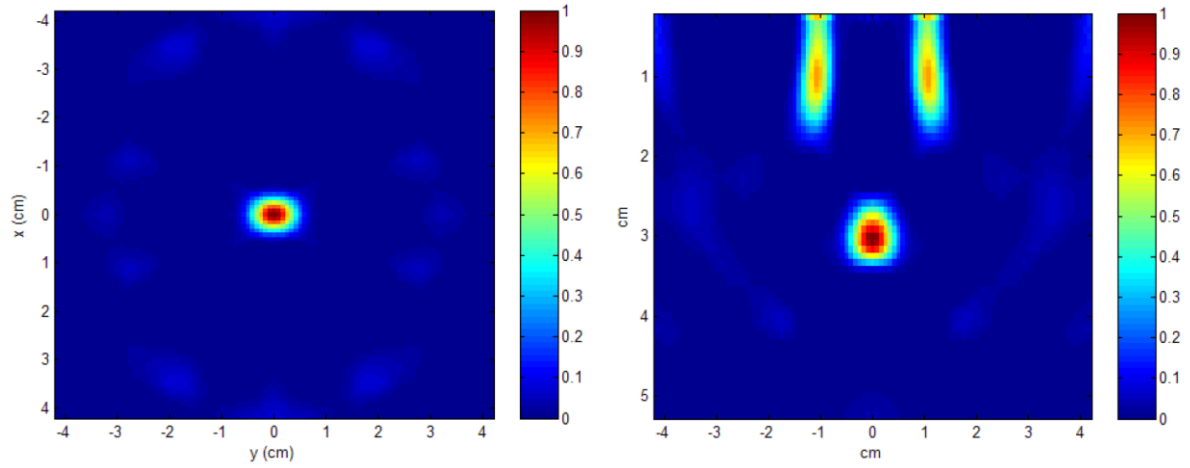

(a) (b)

Figure 5. Tumor detection results: (a) x-y plane result points to the true tumor site at model center, (b) y-z plane result points to true candidate location at 3 cm depth and false skin layer related candidate-locations

purpose, matched-filter bank output signals, obtained for the idealistic homogenous breast tissue with a 5 mm diameter spherical-tumor model, are presented first in Figure 6. To assess such obtained matched-filtering results, it is important to compare the matched-filter output

signals' maxima and their time instants. Of these, normalized maximum value is obtained by normalizing signal to the ideal-case observation while ideal sampling instant is obtained by locating the signal to time origin of the summed-signal observation window. Corresponding results are presented in Table 1. It is clear from these figures and the table that only the output of the filter that is matched to the 5 mm diameter spherical-tumor's Shift&Sum return yields a maximum of 1 at the ideal sampling time, shown as 0 time instant, in both figures. Hence, matched-filter bank clearly points to the 5 mm spherical-tumor existence among all others for the homogenous breast model observation, as expected.

Table 1. Matched-filtering performance comparison for different tumor types in the homogenous breast model

	Spherical (2.5 mm)	Spherical (5.0 mm)	Spherical (7.5 mm)	Cylindrical (3.0 mm)	Cylindrical (4.2 mm)
Matched-filter maximum	6.3	**1**	0.6	1.3	0.6

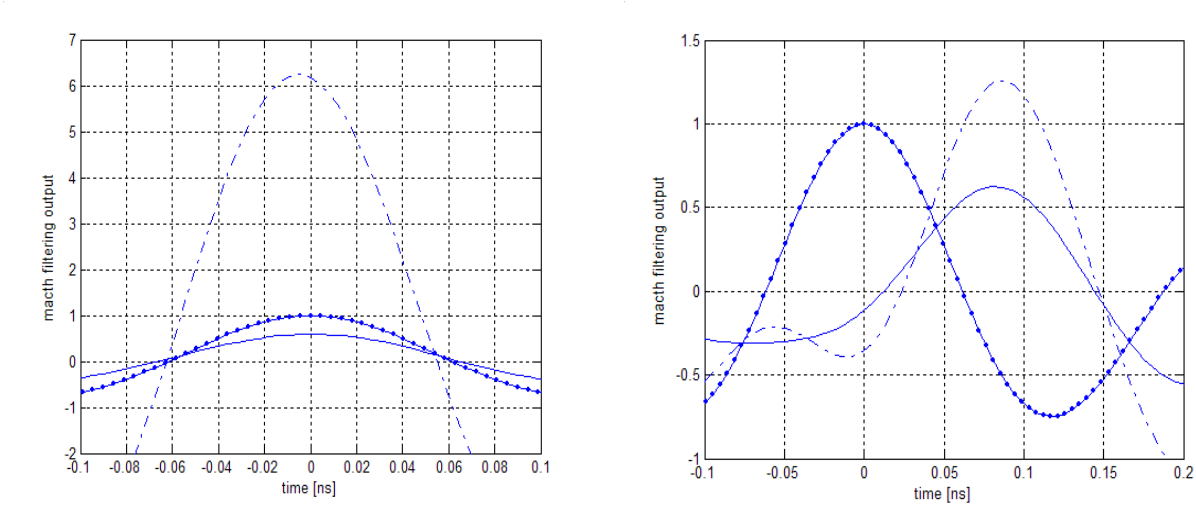

(a) (b)

Figure 6. Matched-filter bank output signals for a 5 mm diameter spherical tumor observed in a homogenous breast tissue model: (a) Dashed line 2.5 mm spherical-tumor filter response, dotted line 5 mm spherical-tumor filter response and solid line 7.5 mm spherical-tumor filter response, (b) Dashed line 3 mm cylindrical-tumor filter response, dotted line 5 mm spherical-tumor filter and solid line 4.2 mm cylindrical-tumor filter response.

Results obtained for the realistic breast model are also presented. This realistic model includes a heterogeneous breast tissue with a variation in the ±10 % range of the reported nominal values along with a 5 mm spherical-tumor buried inside. First set of results, obtained for the quadruple-symmetric heterogeneous model using an antenna-array spatial resolution of 8 mm, are given in Figure 7(a). Here, matched-to-5 mm diameter spherical tumor filter output signals of two candidate points of Figure 5(b), gathered through the tumor detection algorithm, are shown.

Based on the Figure 6 results, the true tumor-location response yields to a maximum which is close to normalized magnitude at the ideal sampling instant compared to that of the false tumor location candidate site. This shows the tumor existence at the true location and is consistent with Shift&Sum result of tumor detection algorithm for two candidate locations as shown in Figure 7(b). Here, some level of clutter that exists after the Shift&Sum process yields a deviation from the ideal matched-filtering observations. Especially high level of clutter, originated from earlier backscatter compared to tumor-related reflection, results in 0.014 ns shift of matched-filter maximum from the ideal sampling instant, shown in Figure 6.

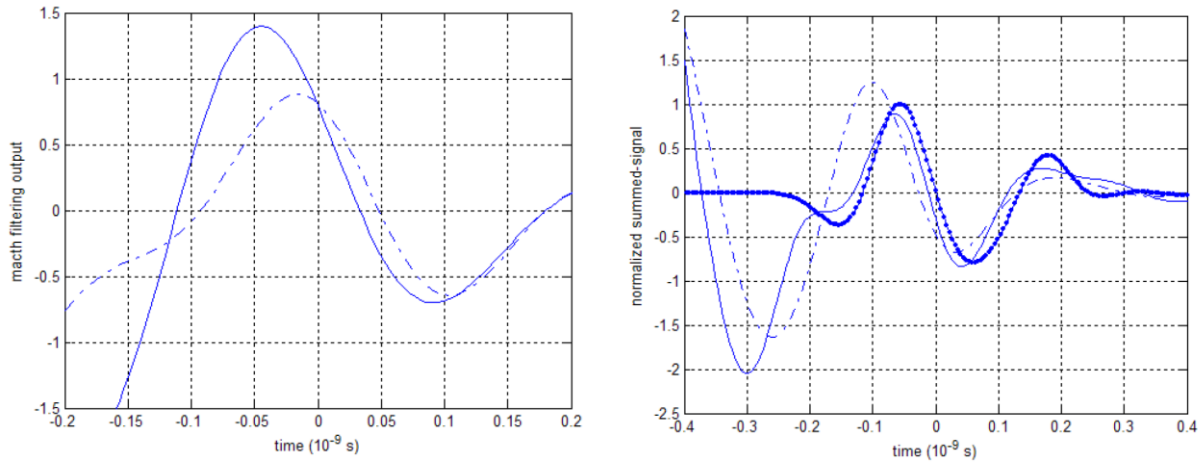

(a) (b)

Figure 7. Preliminary quadruple-symmetric heterogeneous model results: (a) matched-to-5 mm diameter spherical-tumor filter output signals at true tumor location (dashed line) and false tumor location (solid line), (b) output signals of tumor detection (Shift&Sum) algorithm tuned to true tumor location (solid line), false tumor location (dashed line) and ideal homogenous model (dotted line)

To better demonstrate the effect of remaining clutter through the use of Shift&Sum procedure prior to the application of matched-filtering process but on a coarser antenna-array with a spatial resolution of 16 mm, similar matched-filtering results, obtained for reduced heterogeneity with ±1% variation, are shown in Figure 8. In both figures, matched-filter maximums as well as their time instants deviate from that of the ideal homogenous-model results of Figure 3 and 4. Comparison of these results illustrate the performance and efficiency of Shift&Sum procedure in the sense that the tumor detection algorithm performance degrades with reduced number of microwave pulse transmission-reception on antenna-array locations although the experiment is performed for an almost-homogenous breast model with ten times reduced variation.

D. Discussion

Based on the obtained tumor detection results of realistic heterogeneous breast model with reported parameters, a possible tumor site is detectable through the use of Shift&Sum procedure. This algorithm improves the very low level of signal-to-clutter ratio of the microwave observations on the antenna-array locations. Especially back-scatter signals,

originated earlier than that of a possible tumor site, degrade the signal-to-clutter ratio, and the use of Shift&Sum procedure improves this ratio by coherently combining tumor reflections while averaging random backscatter signals caused by breast tissue heterogeneity. Hence, antenna-array spacing is an important parameter for controlling the performance of this procedure. That is, same tumor site is detectable in a heterogenous breast model with ±10% variation for 8 mm antenna-array resolution while this performance drops for a heterogenous model with low breast tissue variation of ±1% but doubled antenna-array spacing of 16 mm.

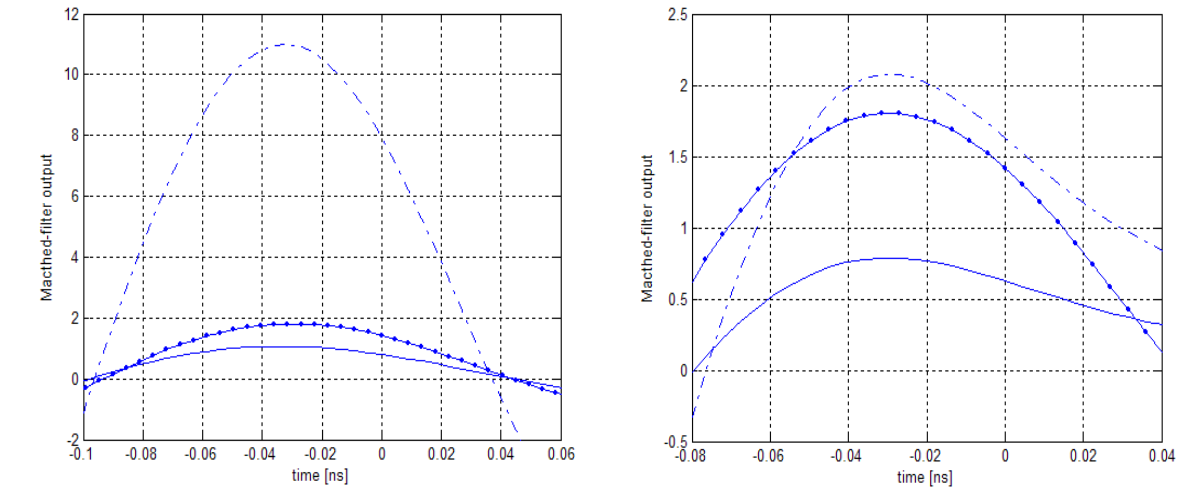

(a) (b)

Figure 8. Matched-filter bank output signals for the response of Shift&Sum procedure focused to real tumor location in a breast-model with reduced heterogeneity of ±1% variation and embedded 5-mm-diameter spherical tumor: (a) dashed line represents matched-to-2.5 mm spherical tumor filter output, dotted line represents matched-to-5 mm spherical tumor filter output, and solid line represents matched-to-7.5 mm spherical tumor filter output, (b) dashed line represents matched-to-3 mm cylindrical tumor filter output, solid line represents matched-to-4.2 mm cylindrical tumor filter output (matched-to-5 mm spherical tumor filter output, represented by dotted line, is also included for comparison)

As a second argument, reference microwave observations, obtained for non-scattering idealistic breast model, are efficient for classifying tumor shape and size that resides at a possible tumor site. For that, five tumors with different morphologic parameters were considered for a general assessment. They were used to construct a Shift&Sum procedure signal bank, and this data were then used to classify the observations of a possible tumor site, detected in a realistic breast model. From the comparison of Figure 6 (a), Figure 7(a) and Figure 8 (a) results, match-filtering approach is effective for tumor morphology classification as long as the clutter in the antenna-array observations can be lowered to a certain degree, and its usage can be expanded with the use of a broader matched-filter bank.

4. Conclusion

Detection of breast tumor existence and its morphologic classification are two important research topics in medical assessment. In this study, use of Shift&Sum procedure, based on antenna-array microwave back-scatter observation signals, is proposed for tumor existence. Once a possible tumor site is detected using this approach, signal-to-clutter ratio enhanced Shift&Sum procedure output signals are then processed through matched-filtering for tumor type classification. The major obstacle in microwave back-scatter based breast tumor detection and related tumor type classification is the clutter that takes places earlier in time than the tumor related reflections. Although Shift&Sum procedure efficiently lowers this clutter, improvement or alternative clutter-removal solutions may be investigated as a future work. As a final note, matched-filter bank can also be extended for a detailed tumor type classification.

Acknowledgements

This study includes the results of the Ph. D. dissertation titled as “A Computational Study of Reconstruction Algorithms for Ultra-Wideband Electromagnetic Pulse Imaging in Tissue” by Emin Argun Oral.

Ethics in Publishing

There are no ethical issues regarding the publication of this study.

Author Contributions

Emin Argun Oral has completed all simulation modelling, experimental studies and preparation of this manuscript under the supervision of Alan V. Sahakian.

References

[1] American Cancer Society. Cancer Facts & Figures 2021; American Cancer Society: Atlanta, GA, USA, 2021. Available online: https://www.cancer.org/research/cancer-facts-statistics/all-cancer-facts-figures/cancer-facts-figures-2021.html (accessed on 21 April 2022)

[2] S. Kwon, S. Lee, “Recent advances in microwave imaging for breast cancer detection”, Int. J. Biomed. Imaging. 2016, 5054912

[3] S.G. Orel, M.D. Schnall, “MR imaging of the breast for the detection, diagnosis, and staging of breast cancer”, Radiology 2001, 220, 13–30

[4] M.A. Aldhaeebi, T.S. Almoneef, H. Attia, O.M. Ramahi, “Near-Field Microwave Loop Array Sensor for Breast Tumor Detection”, IEEE Sens. J. 2019, 19, 11867-11872

[5] B. Bocquet, J. Van de Velde, A. Mamouni, Y. Leroy, G. Giaux, J. Delannoy, D. Delvalee, “Microwave radiometric imaging at 3 GHz for the exploration of breast tumours”, IEEE Trans. Microw. Theory Tech. 1990, 38, 791–793

[6] S. Mouty, B. Bocquet, R. Ringot, N. Rocourt, P. Devos, “Microwave radiometric imaging (MWI) for the characterisation of breast tumours”, Eur. Phys. J. Appl. Phys. 2000, 10, 73–78

[7] P.M. Meaney, M.W. Fanning, D. Li, S.P. Poplack, K.D. Paulsen, “A clinical prototype for active microwave imaging of the breast”, IEEE Trans. Microw. Theory Tech. 2000, 48, 1841–1853

[8] M. Ambrosanio, P. Kosmas, V. Pascazio, “A Multithreshold Iterative DBIM-Based Algorithm for the Imaging of Heterogeneous Breast Tissues”, IEEE Trans. Biomed. Eng. 2018, 66, 509–520

[9] M. Maffongelli, S. Poretti, A. Salvadè, R. Monleone, C. Pagnamenta, A. Fedeli, M. Pastorino, A. Randazzo, “Design and experimental test of a microwave system for quantitative biomedical imaging”, Proceedings of the 2018 IEEE International Symposium on Medical Measurements and Applications (MeMeA), Rome, Italy, 11–13 June 2018; pp. 1–6

[10] S.P. Rana, M. Dey, G. Tiberi, L. Sani, A. Vispa, G. Raspa, M. Duranti, M. Ghavami, S. Dudley, “Machine Learning Approaches for Automated Lesion Detection in Microwave Breast Imaging”, Clinical Data. Sci. Rep. 2019, 9, 10510

[11] O.M. Bucci, G. Bellizzi, A. Borgia, S. Costanzo, L. Crocco, G. Di Massa, R. Scapaticci, “Experimental framework for magnetic nanoparticles enhanced breast cancer microwave imaging”, IEEE Access 2017, 5, 16332–16340

[12] S. C. Hagness, A. Taflove, J. E. Bridges, “Two-Dimensional FDTD Analysis of a pulsed Microwave Confocal System for Breast Cancer Detection: Fixed-Focus and Antenna-Array Sensors,” in IEEE Trans. On Biomed. Eng., vol. 45, no. 12, pp. 1470-1479, Dec. 1998

[13] S. C. Hagness, A. Taflove, J. E. Bridges, “Three-Dimensional FDTD Analysis of a pulsed Microwave Confocal System for Breast Cancer Detection: Design of an Antenna-Array Element,” in IEEE Trans. On Antennas Propagat., vol. 47, no. 5, pp. 783-791, May 1999

[14] X. Li, S. C. Hagness, “A Confocal Microwave Imaging Algorithm for Breast Cancer Detection,” in IEEE Microwave and Wireless Letters, vol. 11, no. 3, pp. 130-132, Mar. 2001

[15] S. Coarsi, A. Massa, M. Pastorino, “Numerical Assessments Concerning a Focused Microwave Diagnostic Method for Medical Applications,” in IEEE Trans. On Microwave Theory and Tech., vol. 48, no. 11, pp. 1815-1830, Nov. 2000

[16] K. R. Foster, and H. P. Schwan, “Dielectric properties of tissues and biological materials: A critical review,” Critical Reviews Biomed. Eng., vol. 17, no. 1, pp. 25-102, 1989

[17] K. R. Foster, and J. L. Schepps, “Dielectric properties of tumor and normal tissues at radio through microwave frequencies,” Journal Microwave Power, vol. 16, no. 2, pp. 107-119, 1981

[18] E. C. Fear, M. A. Stuchly, “Microwave Detection of Breast Cancer,” in IEEE Trans. On Microwave Theory and Tech., vol.48, no. 11, pp. 1854-1863, Nov. 2000

[19] J. Shea, P. Kosmas, B. Van Veen, S. Hagness, “Contrast-enhanced microwave imaging of breast tumours: A computational study using 3D realistic numerical phantoms”, Inverse Probl. 2010, 26, 074009

[20] D. Byrne, M. O’Halloran, M. Glavin, E. Jones, “Data independent radar beamforming algorithms for breast cancer detection”, Prog. Electromagn. Res. 2010, 107, 331–348

[21] D. Byrne, M. Sarafianou, I.J. Craddock, “Compound radar approach for breast imaging”, IEEE Trans. Biomed. Eng. 2017, 64, 40–51

[22] T. Yin, F.H. Ali, C.C. Reyes-Aldasoro, “A robust and artifact resistant algorithm of ultra-wideband imaging system for breast cancer detection”, IEEE Trans. Biomed. Eng. 2015, 62, 1514–1525

[23] S. Kubota, X. Xiao, N. Sasaki, Y. Kayaba, K. Kimoto, W. Moriyama, T. Kozaki, M. Hanada, T. Kikkawa, “Confocal imaging using ultra wideband antenna array on Si substrates for breast cancer detection”, Jpn. J. Appl. Phys. 2010, 49, 097001

[24] I. Ünal, B. Türetken, C. Canbay, “Spherical Conformal Bow-Tie Antenna for Ultra-Wide Band Microwave Imaging of Breast Cancer Tumour”, Appl. Comput. Electromagn. Soc. J. 2014, 29

[25] G.N. Bindu, S.J. Abraham, A. Lonappan, V. Thomas, C.K. Aanandan, K. Mathew, “Active microwave imaging for breast cancer detection”, Prog. Electromagn. Res. 2006, 58, 149–169

[26] E. C. Fear, X. Li, S. C. Hagness, M. A. Stuchly, “Confocal Microwave Imaging for Breast Cancer Detection: Localization of Tumors in Three Dimensions,” IEEE Trans. On Biomed. Eng., vol. 49, no. 8, pp. 812-822, Aug. 2002